Natural Hazards
https://doi.org/10.1007/s11069-022-05606-2

ORIGINAL PAPER

Alert threshold assessment based on equivalent displacements for the identification of potentially critical landslide events

Alessandro Valletta[1] · **Andrea Carri**[2] · **Andrea Segalini**[1]

Received: 17 May 2022 / Accepted: 2 September 2022

Abstract
Over the past years, the growing number of natural hazards all over the world has led to an increasing focus on activities aimed at studying and controlling the occurrence of these phenomena. In this context, monitoring systems have become a fundamental component for Landslide Early Warning Systems, allowing to understand the evolution of these processes and assess the need for dedicated mitigation measures. This result is achieved thanks to several technological advancements that led to the introduction of more accurate and reliable sensors, as well as automatic procedures for data acquisition and elaboration. However, despite these improvements, the data interpretation process is still a challenging task, in particular when it comes to the identification of critical events and failure forecasting operations. This paper presents a methodology developed to assess if a potentially critical event is displaying a significant deviation from previously sampled data, or if it could be classified as a false alarm. The process relies on the definition of a threshold value based on the landslide behavior preceding the event of interest. In particular, the reference value derives from the evaluation of equivalent displacements, defined as the displacements previously observed in a time interval equal to the one showed by the potentially critical event. This paper reports a series of examples referring to different case studies, involving both false alarms and real collapses, underlining the effectiveness of the proposed model as a useful tool to evaluate the landslide behavior with a near-real-time approach.

Keywords Landslide · Monitoring · Displacement · Early warning system · Alert threshold

✉ Alessandro Valletta
alessandro.valletta@unipr.it

[1] Department of Engineering and Architecture, University of Parma, Parco Area delle Scienze 181/a, 43124 Parma, Italy

[2] ASE—Advanced Slope Engineering S.r.l., Via Robert Koch 53/a, Fraz. Pilastrello, 43123 Parma, Italy

Published online: 15 September 2022

1 Introduction

In the landslide risk management framework, Early Warning Systems (EWS) represent an effective and feasible option, especially in those cases where structural measures are not viable due to economical or practical reasons (Londoño 2011). The popularity of these approaches can be attributed to several factors, including their lower economic costs and environmental impact, the advantages deriving from the introduction of new technologies for landslide monitoring, and the increased availability of reliable databases to calibrate the warning models (Barla and Antolini 2016; Pecoraro et al. 2019).

According to the definition provided by the United Nations International Strategy for Disaster Reduction (UNISDR), early warning systems are defined as "the set of capacities needed to generate and disseminate timely and meaningful warning information to enable individuals, communities and organizations threatened by a hazard to prepare and to act appropriately and in sufficient time to reduce the possibility of harm or loss" (UNISDR 2009). In a more recent report focused on the terminology related to disaster risk deduction, the following definition for EWS was included: "An integrated system of hazard monitoring, forecasting and prediction, disaster risk assessment, communication and preparedness activities systems and processes that enables individuals, communities, governments, businesses and others to take timely action to reduce disaster risks in advance of hazardous events" (United Nations 2016).

Several authors over the years have proposed a description of the general structure of an EWS, aiming to summarize the key elements that should always be included in the design process of a landslide-oriented Early Warning System. According to UNISDR, complete and effective EWS should include four components: risk knowledge, monitoring and warning service, dissemination and communication, and response capability (UNISDR 2006). Each one of these elements plays an essential role, and a weakness in a single one of these could result in the failure of the entire system. Di Biagio and Kjekstad (2007) proposed an alternative approach, using a flow diagram to highlight four main activities: monitoring, analysis and forecasting, warning, and response. According to the authors, the EWS effectiveness depends especially on the identification, monitoring, and measurement of the events preceding a landslide occurrence. In particular, the precursors identification is essential for the correct choice of the most appropriate monitoring sensors. Starting from these two approaches, Intrieri et al. (2013) described the EWS structure as a balanced combination of four components: design, monitoring, forecasting, and education. The third phase, involving the forecasting and alert threshold assessment operations, is regarded by the authors as the most critical element of a Landslide Early Warning System (LEWS). In particular, they underline the problem represented by false alarms, which can be reduced but never completely eliminated from the early warning process. Calvello et al. (2015) combined several contributions on this topic, proposing a new schematization in the form of a wheel-like diagram. This approach underlines the necessity of a synergic connection between technical and social skills, with the objective of defining efficient processes and making the EWS an effective risk reduction tool. Moreover, it introduces the temporal continuity of the activities to be undertaken for updating the system during its operational life. Another recent LEWS scheme was presented by Fathani et al. (2016), with the main purpose to introduce an integrated methodology to be used as a standard for the definition of community-based EWS. To achieve this objective, the proposed approach starts from the UNSIDR definition and expands it by introducing seven sub-systems to better describe the EWS creation process.

As previously noted, the processes for the definition of alert levels and thresholds are among the most difficult to entail. Because of their own nature, these should be determined with the intent to represent a critical event in the context of the studied phenomenon, i.e., a condition that may trigger a landslide when exceeded (Guzzetti et al. 2007). For what concerns the landslide monitoring framework, these occurrences are usually associated with slope collapses generated by a situation of irreversible instability of the studied element. In many cases, the threshold assessment process is completely empirical, relying on expert judgment and available monitoring data, and provides values suitable only for the specific landslide for which they are originally defined (Intrieri et al. 2019). Numerical modeling is another possible approach to assess warning levels for a specific landslide. These methods aim to compare displacements measured by monitoring tools installed on-site with values obtained from a reference model. If properly designed and calibrated, the model should be able to represent the behavior of the real slope, thus allowing the definition of one or more thresholds corresponding to different stages of the monitored slope evolution over time (Huggel et al. 2010; Thiebes et al. 2014; Festl and Thuro 2016; Du and Wang 2016; Newcomen and Dick 2016; Zhao et al. 2020; López-Vinielles et al. 2021). This approach can be indeed highly effective, although the large number of components to take into account in the modeling process makes it a quite challenging and time-consuming task. In more recent time, technological improvements regarding the computational ability of modern computers, together with the increased availability of powerful software able to process advanced algorithms, have boosted significantly the research activity in this specific field. As a result, several authors have presented new studies and methodologies based on a wide range of different approaches, such as algorithms relying on Artificial Intelligence (Di Napoli et al. 2020; Guardiani et al. 2021; Liu et al. 2021; Ma et al. 2021) and Neural Networks (Chen et al. 2015; Prakash et al. 2021; Zhang et al. 2022).

On the other hand, other methodologies have been developed over the years focusing on the possibility of creating a more general procedure, not strictly dependent from a specific case study. In these cases, the design process is based on failure forecasting methods (Crosta and Agliardi 2002; Manconi and Giordan 2016; Carlà et al. 2018; Valletta et al. 2020), or derives from a solid observational basis (Brox and Newcomen 2003; Xu et al. 2011). Due to their notable degree of exportability, these methodologies can be integrated in different slope-scale EWS. Nonetheless, they tend to share the same issues affecting the methods from which they derive and should not be used in isolation with a "closed box" approach. In fact, at present, the most reliable approach appears to be the integration of more than one method in order to have a more complete description of the phenomenon (Intrieri and Gigli 2016).

2 Materials and methods

The methodology here presented relates to this concept, aiming to exploit the availability of a large amount of information regarding the past movements of the monitored landslide as a comparison with determine the impact of newly recorded displacements on the slope stability conditions. In particular, the approach was designed with the main purpose to identify the occurrence of a specific category of false alarms. These consist of events displaying a data trend geometrically compatible with an accelerating pattern, while featuring a displacement magnitude which does not correspond to a critical occurrence if compared to previously observed occurrences. As previously noted, the introduction of new

technologies in the geotechnical field has notably increased the monitoring systems reliability and sampling rate, thus making them able to provide a considerable amount of information over time. On this basis, the proposed approach seeks to exploit the availability of available monitoring data to assess one or more alert levels not only for any particular case study, but also specifically for each single event identified by the monitoring instrumentation. Moreover, the methodology was developed trying to balance computational complexity and results reliability, designing a procedure conceptually easy to understand and implement, while being able to provide meaningful information for early warning purposes at the same time.

The process to define the alert threshold value can be divided into a series of consecutive steps, starting from the acquisition of landslide displacement data. When the elaboration software detects a potentially critical event, it extracts the corresponding dataset and evaluates the displacement generated d_0^* and its duration t^*. The event identification can be performed starting from available monitoring data, and the corresponding dataset is expected to follow an increasing trend in the displacement–time plot. The authors developed a multi-criteria algorithm specifically designed for the identification of the onset-on-acceleration (OOA) and the subsequent acceleration phase, relying on a drop-down procedure composed of four steps that are applied to each single data sample to detect specific variations in the landslide behavior (Valletta et al. 2021). The method is based on the hypothesis that the monitored landslide would display a transition from a linear to a nonlinear behavior, corresponding, respectively, to a constant and increasing displacement rate. Therefore, if the elaboration process identifies a trend that fulfils all criteria, it is possible to define a displacement dataset representing an increasing velocity over time.

Taking as a reference the date t_x of the first point d_x (i.e., the OOA) included in the dataset, the software retrieves all monitored data sampled by the same sensor during the 30 days preceding the event. These values are going to serve as a term of comparison for the event identified at the previous step, using t^* as the time interval reference for the calculation of equivalent displacements. This term defines the slope displacements measured before the event occurrence and developed over a time interval equal to the one showed by the potentially critical event. By doing this, the algorithm produces a series of displacements d_n^* generated over the same time interval t^*. Table 1 reports an example of this procedure for a dataset composed of six displacement values, under the hypothesis of constant sampling frequency during the monitoring activity (i.e., the time interval is equal for datasets featuring the same number of values).

Therefore, it is possible to assess an alert threshold d_{th}^* based on the values of mean μ_S and standard deviation σ_S referred to the dataset of the equivalent displacement previously calculated:

Table 1 Evaluation of equivalent displacement values for a potentially critical event composed of six data

Dimension of the dataset referred to the event of interest = 6	
Event identified	$d_0^* = d_x - d_{x-5}$
Equivalent displacement 1	$d_1^* = d_{x-1} - d_{x-6}$
Equivalent displacement 2	$d_2^* = d_{x-2} - d_{x-7}$
Equivalent displacement 3	$d_3^* = d_{x-3} - d_{x-8}$
…	…
Equivalent displacement n	$d_n^* = d_{x-n} - d_{x-5-n}$

$$d^*_{\mathrm{th}} = \mu_S + 3\sigma_S \tag{1}$$

Finally, it is possible to compare this outcome with the displacement d^*_0, in order to verify if the event generated a displacement with a magnitude similar to values previously observed during the considered time period, or if the resulting values overcome the alert threshold, thus indicating an unusually intense phenomenon. The flow diagram reported in Fig. 1 summarizes the procedure outlined above.

The reference time interval for the evaluation of equivalent displacements, and the related threshold value, was assessed on the basis of a series of considerations regarding the monitoring activity of a landslide, and after calibrating the model on several datasets sampled with automatic instrumentation installed in different sites of interest. The main observation concerns the number of monitoring data to be included in the dataset, which should be large enough to allow an appropriate definition of a typical trend of the landslide before the event occurrence. In fact, by choosing a too short time interval, the threshold fluctuations induced by single equivalent displacement would be too prominent, resulting in an unreliable threshold definition process. At the same time, taking into account a very long time interval for this operation would force to wait a prolonged time period after the installation of the monitoring tools, severely limiting the effectiveness of the warning system. The introduction of automatic instrumentation able to achieve sampling frequencies of hours, and even minutes, could potentially play an important role when addressing this issue. However, it should be also taken into account that a very high number of data collected in a short time period could not provide a comprehensive representation of the general behavior of the monitored landslide. The time period here proposed was chosen by taking into consideration these remarks together with empirical observations coming from the application of the methodology to different datasets. Nonetheless, while the 30-day interval provided positive results during the calibration and testing phases, the possibility to select a more appropriate time window according to on-site observations in specific case studies should not be entirely discarded.

Figure 2 reports four examples obtained during the calibration process. Each plot shows the equivalent displacement evaluated according to the previously discussed procedure and displays the alert threshold value evaluated by considering a varying number of monitoring data. The first three datasets relate to case studies where the sampling frequency was set

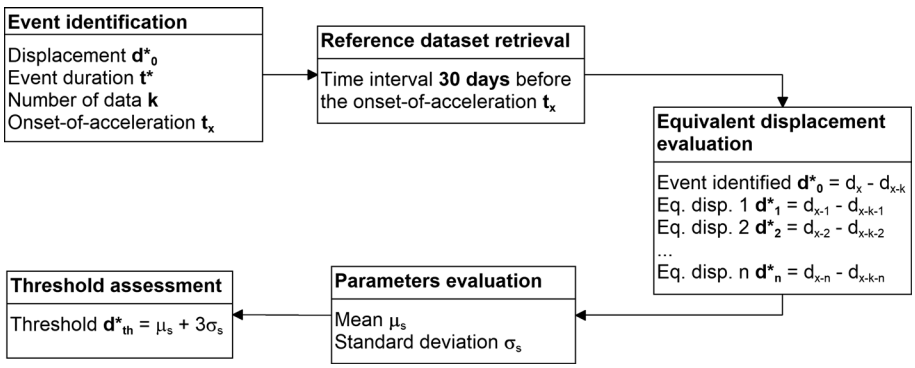

Fig. 1 Flow diagram summarizing the main steps for the assessment of an alert threshold based on equivalent displacements

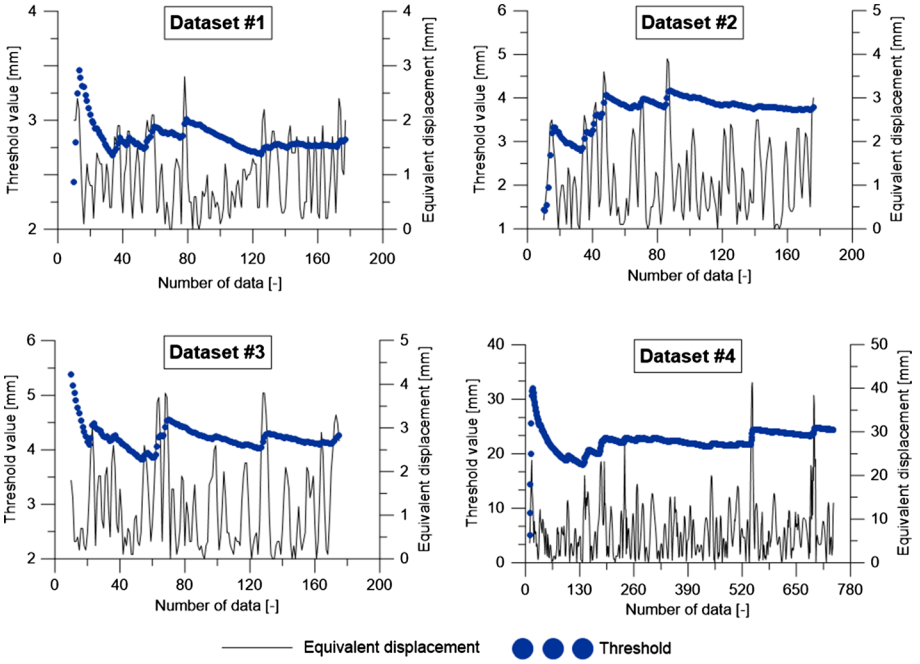

Fig. 2 Four examples evidencing the alert threshold value variation according to the number of monitoring data taken into consideration in the calculation process

to six readings per day, resulting in a total number of monitoring values equal to 180 for each month. The 4th dataset refers to a monitoring system configured with an hourly sampling frequency, thus producing a 720-point dataset. These examples show how the threshold experiences very prominent variations when its assessment relies on smaller datasets and reaches a more stable value when more data are added to the calculation process. It is worth noting that the presence of some peaks in the equivalent displacement dataset is still able to influence the threshold value even if large datasets are taken into account, as can be observed for example in dataset #3 and #4. However, this should not be seen as an issue, since higher equivalent displacement values are an indication of the occurrence of past events generating more noticeable slope movements, which should not be neglected when assessing the standard behavior of the monitored landslide.

3 Results and discussion

The threshold assessment process has been applied to a wide range of dataset recorded in real-time, working in synergy with the previously mentioned methodology designed to identify accelerating trends in landslide displacements. In the following sections, three different case studies involving a total of four events are described, in order to present some examples of the methodology application and outcomes in a real scenario. The examples provided in this paper include also a back-analysis performed on a case

study where the detected event led to an actual collapse of the monitored slope (thus representing a "true" positive in terms of early warning).

3.1 Case study #1

The first case study involves the monitoring activity of a slope located in Southern Italy, where a series of instability phenomena were identified after the construction of a viaduct connected to a State Road crossing the area. As a consequence, a multi-parameter monitoring system was installed in order to study the phenomenon evolution, focusing on its interaction with the infrastructure. The instrumentation included seven Vertical Array automatic inclinometers, based on MUMS (Modular Underground Monitoring System) technology developed and produced by ASE S.r.l. (IT). The instrumentation is an array composed of different nodes (named Links) connected by a quadrupole electrical and an aramid fiber cables in order to form an arbitrary long chain of sensors (Segalini et al. 2014; Carri et al. 2015). It can be equipped with 3D MEMS, electrolytic cell, piezometer, thermometer, and other typologies of sensors, while a dedicated data logger connected to the Array automatically queries each different Link. The on-site location and composition of each array should be carefully considered in the project phase with the aim of providing a comprehensive description of the landslide, focusing on different sectors of the monitored slope. This aspect is essential for any monitoring activity intended for early warning purposes. For this case study, the length and composition of each Array varied according to the on-site position of the equipment. The monitoring system included also three Piezo Arrays, each one integrating a series of analog piezometers to record the pore pressure and water level variation over time; seven tilt meters, installed on the viaduct piles to control the stability conditions of the structure; three barometers to monitor the atmospheric pressure; and a rain gauge for the measurement of rainfalls in the area. Table 2 summarizes the main features of the monitoring system.

On 24 September 2020, the elaboration software reported the presence of an accelerating pattern detected by Vertical Array DT0074 in correspondence of Tilt Link 15, located at a depth of 16 m (Fig. 3). The automatic routine for the determination of the onset-of-acceleration identified the beginning of the event at 06:13. After the definition of the dataset of interest, the first step for the alert level assessment process involves the determination of the displacement generated by the event itself and the corresponding time interval. In this case, since this device was set to sample new data every 6 h, the monitoring data showed a displacement 1.5 mm over a time period of approximately 30 h.

The subsequent operation consists of retrieving monitoring data from the 30 days preceding the event of interest, in order to assess the equivalent displacements and the correlated threshold. Taking the OOA as a reference, displacements recorded since 24 August 2020 06:13 were retrieved in this phase. Each equivalent displacement value is computed by considering a time interval equal to the one obtained from the event, resulting in 118 equivalent displacements. By exploiting the mean and standard deviation values calculated on this dataset, respectively, equal to 0.74 and 0.56 mm, the alert threshold based on equivalent displacements is equal to 2.5 mm (Table 3). As a result, it is possible to state that the identified event does not display a concerning behavior if compared to previously sampled monitoring data, since the corresponding displacement does not overcome the computed threshold (Fig. 4).

Table 2 Features of the automatic multi-parameter monitoring system installed near a viaduct located in Southern Italy to control the evolution of an instability phenomenon and its interaction with the structure

Array ID (−)	Installation date (dd/mm/yyyy)	Array typology (−)	Sensors number and typology (−)	Array length (m)
DT0070	21/07/2017	Vertical Array	15 × Tilt Link HR 3D V	35.00
DT0071	27/07/2017	Piezo Array	7 × Piezo Link 1 × Baro Link	35.00
DT0072	29/07/2017	Vertical Array	30 × Tilt Link HR 3D V 13 × Piezo Link	70.00
DT0073	23/08/2017	Vertical Array	15 × Tilt Link HR 3D V 7 × Piezo Link	35.00
DT0074	29/07/2017	Vertical Array	15 × Tilt Link HR 3D V	35.00
DT0075	28/07/2017	Piezo Array	6 × Piezo Link 1 × Baro Link	35.00
DT0076	26/07/2017	Vertical Array	15 × Tilt Link HR 3D V	35.00
DT0077	23/08/2017	Piezo Array	6 × Piezo Link 1 × Baro Link	35.00
DT0078	21/07/2017	Klino Array	7 × Klino Link HR	–
DT0090	30/03/2018	Vertical Array	20 × Tilt Link HR 3D V	60.00
DT0091	30/03/2018	Vertical Array	30 × Tilt Link HR 3D V	70.00
LOC0035	28/07/2017	Rain Array	1 × Rain Gauge	–

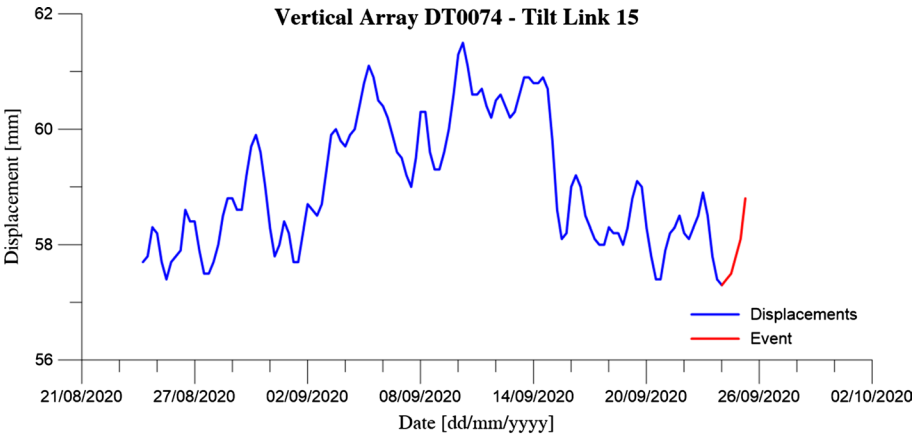

Fig. 3 Displacement values measured by Vertical Array DT0074—Tilt Link 15, referred to the event with OOA on 24/09/2020 06:13, and to the 30 days preceding the event itself

3.2 Case study #2

The second case study deals with the monitoring of a slope located in Southern Italy, crossed by a high-speed railway tunnel currently under construction. After the identification of a quiescent landslide in the area, it was decided to install an automatic monitoring system with the objective of verifying the design hypotheses and control the

Table 3 Characteristics of the DT0074 Tilt Links and the datasets involved in the analysis, together with the displacement generated by the event and the equivalent displacement threshold

Tilt Link ID	Depth (m)	Dataset dimension k	Displacement generated d_0^* (mm)	Mean μ_s (mm)	Standard deviation σ_s (mm)	Equivalent displacement threshold d_{th}^* (mm)
15	16.00	5	1.5	0.74	0.56	2.5

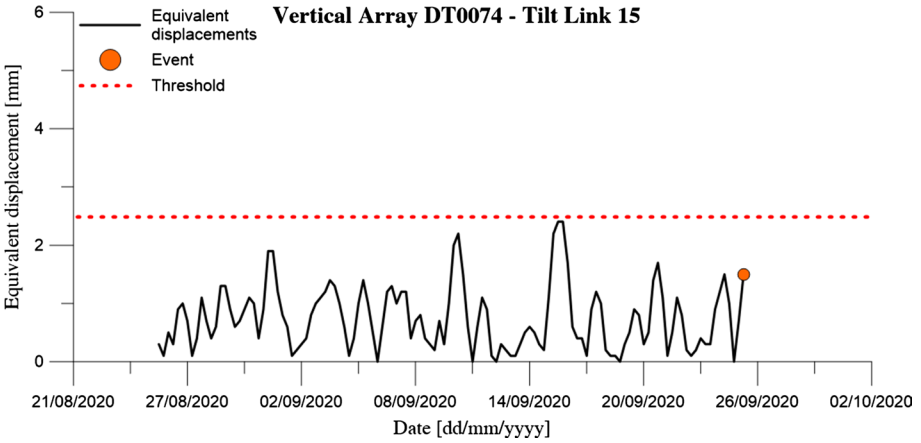

Fig. 4 Graphical representation of equivalent displacements referred to the event of interest, the time period of 30 days preceding the event itself, and the threshold evaluated from these values for DT0074—Tilt Link 15

deformations induced by the excavation works. The monitoring system included a total of four Vertical Array automatic inclinometers, featuring different lengths and number of sensors. Interspace between Links also varied depending on their vertical position, with a distance of 2 m between each node in the supposedly stable area, reducing to 0.5 m in proximity of the sliding surface for an increased degree of detail in the phenomenon description. Additionally, the system comprises four Piezo Arrays, each one composed of two analog piezometers, to record the water level variations over time. The characteristics of each Array are summarized in Table 4.

During the entire monitoring period, all Vertical Arrays evidenced a relevant degree of activity of the monitored site, even without displaying any significant evidence of critical instabilities taking place in the area of interest. For this case study, two events are going to be analyzed, involving two different Arrays in May 2020 and August 2020. Datasets recorded by each Tilt Link that identified an unexpected displacement trend were processed with the algorithm previously detailed, assessing an equivalent

Table 4 Features of the automatic monitoring system installed to control slope displacements and water level variations of a landslide located in Southern Italy

Array ID (−)	Installation date (dd/mm/yyyy)	Array typology (−)	Sensors number and typology (−)	Array length (m)
DT0004	18/02/2020	Piezo Array	2 × Piezo Link	45.00
DT0111	23/01/2020	Vertical Array	73 × Tilt Link V	69.00
DT0005	18/02/2020	Piezo Array	2 × Piezo Link	31.70
DT0112	24/01/2020	Vertical Array	81 × Tilt Link V	80.00
DT0006	18/02/2020	Piezo Array	2 × Piezo Link	52.00
DT0113	14/01/2020	Vertical Array	66 × Tilt Link V	80.00
DT0007	22/01/2020	Piezo Array	2 × Piezo Link	30.00
DT0114	24/01/2020	Vertical Array	31 × Tilt Link V	30.00

displacement threshold to verify how the event magnitude compared to the landslide's past behavior.

The first event here analyzed was detected on 13 August 2020, when the elaboration software indicated the presence of an upward trend in a six-point dataset sampled by Vertical Array DT0112—Tilt Link 48, located 17.50 m below the ground level. The algorithm defined the onset-of-acceleration for the event at 21:51 of the previous day (Fig. 5). According to this information, displacements recorded since 12 July 2020 21:51 were retrieved for the alert threshold assessment procedure. As a result, a total of 184 equivalent displacements were computed by taking as a reference the time interval obtained from the event, i.e., 24 h. Finally, the algorithm evaluated the mean and standard deviation values for the dataset, obtaining an alert threshold equal to 2.9 mm.

The outcomes of this operation are summarized in Table 5, while Fig. 6 presents a graphical comparison between the equivalent displacements and the threshold computed at the previous step. It is possible to observe how the resulting value referred to the event of interest is comparable to previously recorded displacements, not overcoming the threshold value. It is also worth noting that equivalent displacements evaluated for this event do not show any significant peak in the reference time period.

The second event here analyzed was recorded by Vertical Array DT0113 on 24 May 2020, approximately four months after its installation. In this case, the movement detected by the instrumentation was recorded by two Links, namely Tilt Links 43 and 55, placed, respectively, at a depth of 12.50 and 6.50 m. The datasets identified by the software were composed of five monitoring values each, and the beginning of the accelerating phase was set at 04:37. Analyzing the available monitoring data, it is possible to notice a strong similarity between the trends displayed in Figs. 7 and 8, representing the slope displacements for Tilt Link 43 and Tilt Link 55, respectively. Since these values refer to cumulative displacements, it could be assumed that a single movement located at a lower depth influenced the behavior of both Links.

Following the retrieval of displacement data starting from 24 April 2020 04:37, two datasets of 185 equivalent displacements were obtained for the analysis. The operations relating to the evaluation of the displacement generated by the event, the extraction of

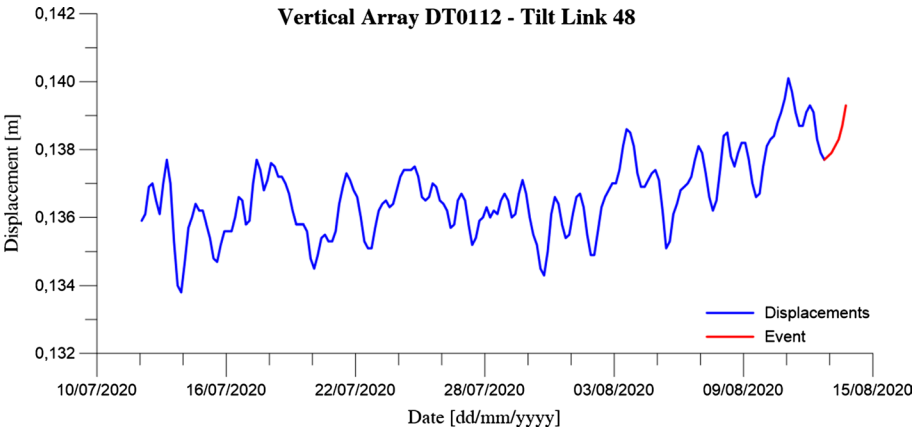

Fig. 5 Displacement values measured by Vertical Array DT0112—Tilt Link 48, referred to the event with OOA on 12/08/2020 21:51, and to the 30 days preceding the event itself

Table 5 Characteristics of the DT0112 Tilt Links and the datasets involved in the analysis, together with the displacement generated by the event and the equivalent displacement threshold

Tilt link ID	Depth (m)	Dataset dimension k	Displacement generated d_0^* (mm)	Mean μ_s (mm)	Standard deviation σ_s (mm)	Equivalent displacement threshold d_{th}^* (mm)
48	18.00	6	1.6	0.99	0.64	2.9

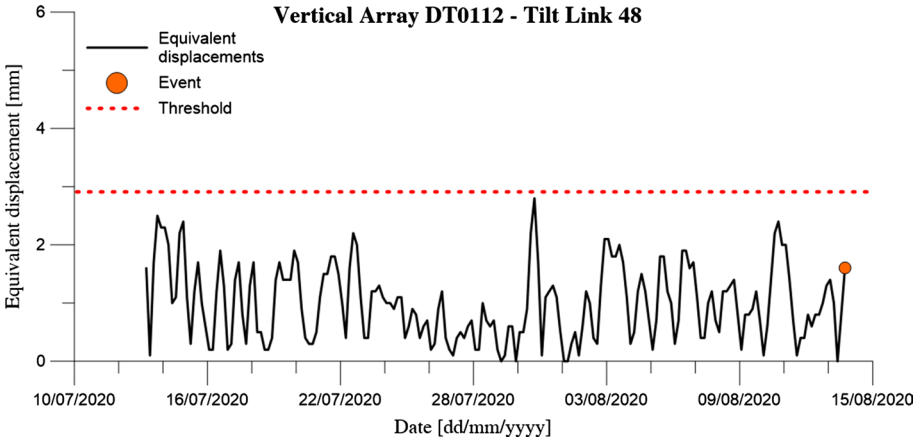

Fig. 6 Graphical representation of equivalent displacements referred to the event of interest, the time period of 30 days preceding the event itself, and the threshold evaluated from these values for DT0112—Tilt Link 48

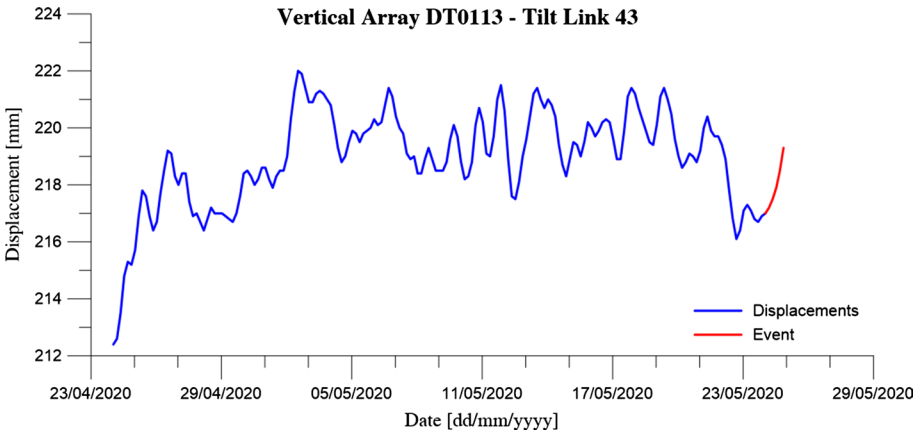

Fig. 7 Displacement values measured by Vertical Array DT0113—Tilt Link 43, referred to the event with OOA on 24/05/2020 04:37 AM, and to the 30 days preceding the event itself

equivalent displacements from previous monitoring data, and the threshold assessment, are summarized in Table 6. All Vertical Arrays on this specific site were set on a sampling rate of 4 h, recording six monitoring values each day. Therefore, since each dataset includes five velocity values, the time interval to evaluate the equivalent displacements for this example is equal to 20 h.

Figures 9 and 10, referring, respectively, to Tilt Link 43 and 55, present a graphical visualization of the analysis outcomes, evidencing how the detected event did not cause a displacement significant enough to overcome the threshold values assessed for the two Links. As seen in the previous case, it is quite easy to notice how the event entity does not appear to be significantly higher than other equivalent displacements, therefore

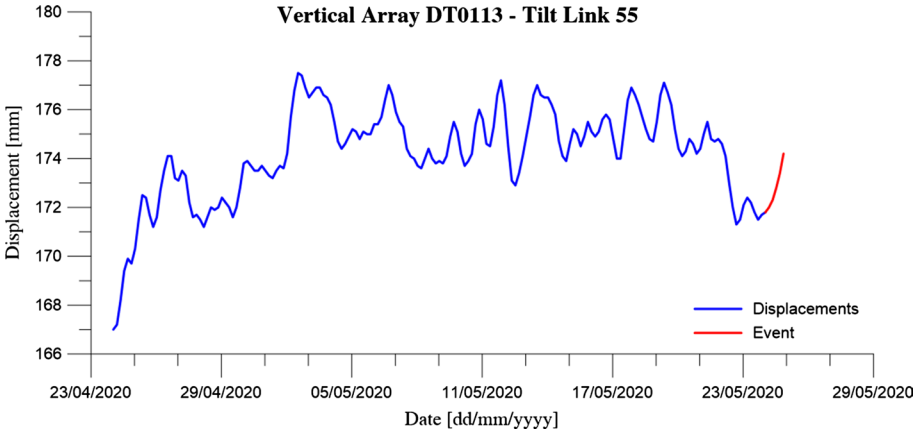

Fig. 8 Displacement values measured by Vertical Array DT0113—Tilt Link 55, referred to the event with OOA on 24/05/2020 04:37 AM, and to the 30 days preceding the event itself

Table 6 Characteristics of the DT0113 Tilt Links and the datasets involved in the analysis, together with the displacement generated by the event and the equivalent displacement threshold

Tilt link ID	Depth (m)	Dataset dimension k	Displacement generated d_0^* (mm)	Mean μ_s (mm)	Standard deviation σ_s (mm)	Equivalent displacement threshold d_{th}^* (mm)
43	12.50	5	2.3	1.14	0.93	3.9
55	6.50	5	2.4	1.20	1.00	4.2

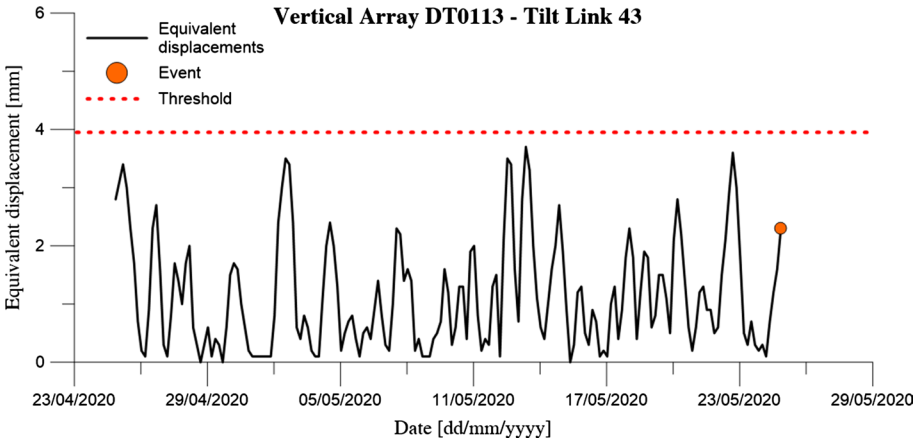

Fig. 9 Graphical representation of equivalent displacements referred to the event of interest, the time period of 30 days preceding the event itself, and the threshold evaluated from these values for DT0113—Tilt Link 43

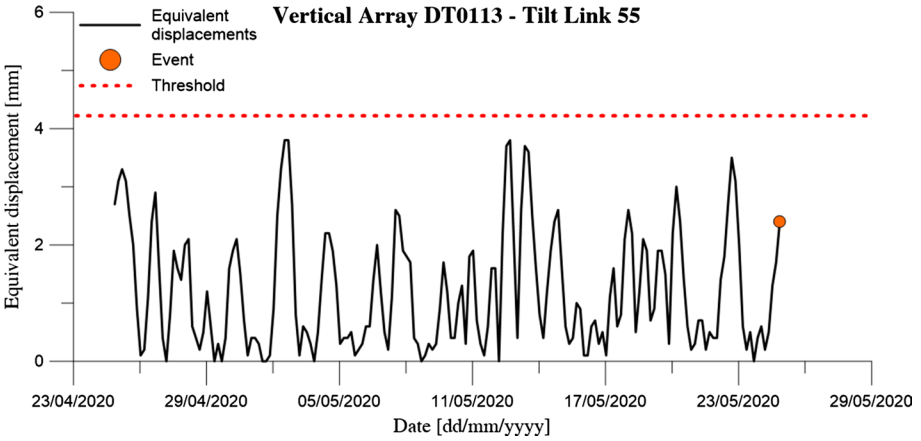

Fig. 10 Graphical representation of equivalent displacements referred to the event of interest, the time period of 30 days preceding the event itself, and the threshold evaluated from these values for DT0113—Tilt Link 55

representing an occurrence where the early warning elaboration was triggered only by the geometric pattern of monitoring data. Moreover, a strong similarity in displacement trends for the Tilt Links considered for this analysis can be observed from available graphs. Since these values are obtained from cumulative displacements, it is possible to assume that both Links were influenced by a common movement located at a lower depth.

3.3 Case study #3

The third case study here discussed refers to the monitoring of a landslide, located in Central Italy, that persists on the construction site of a state road connecting the Adriatic and Tyrrhenian Seas, through Abruzzo and Molise regions. The site is affected by the presence of several landslides in the western sector of the area of interest, showing fast kinematics and sliding surfaces at a depth between 8 and 10 m, with other instabilities appearing in the first meters of material in the Eastern areas. Following a series of preliminary surveys evidencing further problems related to settlements and damages to pre-existing instrumentation, a MUMS-based monitoring system was designed, with a total of nine Vertical Arrays installed on site over approximately 4 years starting from the end of 2016. Each Array featured a different number of Tilt Link HR 3D V, equipped with 3D MEMS and electrolytic tilt sensors, and customized interspace between nodes, as in Table 7.

The event here analyzed, extensively discussed in Segalini et al. (2019), occurred in March 2017, some months after the installation of the Vertical Array DT0014. At that time, DT0014 was the only automatic monitoring device present on site, and the acquisition process was set on a sampling frequency of 1 h. Starting from the end January 2017, the inclinometer recorded a series of displacements involving the first six meters of soil, with some datasets activating the early warning criteria implemented in the software. The phenomenon evolved over the following weeks, leading to a major displacement recorded on March 8th that damaged the Array, partially compromising its functionality. The event was

Table 7 Features of the monitoring system installed to control the slope displacements of a landslide located near a State Road in Central Italy

ID (−)	Installation date (dd/mm/yyyy)	Array typology (−)	Sensors number and typology (−)	Array length (m)
DT0014	18/11/2016	Vertical Array	50 × Tilt Link HR 3D V	35.00
DT0065	07/09/2017	Vertical Array	48 × Tilt Link HR 3D V	35.00
DT0094	19/09/2018	Vertical Array	34 × Tilt Link HR 3D V	69.00
DT0095	18/09/2018	Vertical Array	47 × Tilt Link HR 3D V	95.00
DT0096	20/09/2018	Vertical Array	55 × Tilt Link HR 3D V	111.00
DT0097	19/09/2018	Vertical Array	33 × Tilt Link HR 3D V	66.00
DT0119	11/11/2020	Vertical Array	50 × Tilt Link HR 3D V	100.00
DT0120	14/11/2020	Vertical Array	50 × Tilt Link HR 3D V	100.00
DT0121	13/11/2020	Vertical Array	50 × Tilt Link HR 3D V	100.00

identified by the elaboration software, which issued a series of alert messages to authorities responsible of the monitoring activity.

Ultimately, MUMS inclinometer DT0014 became completely inactive on March 13th due to excessive deformations. In the following days, an on-site inspection confirmed the landslide occurrence, highlighting the presence of a complex dynamic featuring several failures and scarps, settlements, and displacements (Fig. 11). Additionally, an in-depth check of the conditions of previously installed instrumentation reported severe damage caused by the event (e.g., inaccessible inclinometer casings).

It should be noted that only an early version of acceleration criterion was active during the monitoring activity; therefore, no alert threshold based on equivalent displacements was available at the time of the event occurrence. Therefore, a back-analysis was performed on the datasets referring to the displacement observed on 08 March 2017, in order to apply the newly developed methodology to a real case critical scenario. In particular, the sudden increase in displacement rates was identified by Tilt Links 93 and 95, respectively, located 2.5 and 1.8 m below ground surface. For both Links, the analysis returned a seven-point velocity dataset with the onset-of-acceleration at 02:28 of March 8th. By looking at both Figs. 12 and 13, it is possible to notice that a portion of the increasing displacement trend was not included in the dataset of the event. This could potentially be attributed to the criteria integrated in the algorithm for the identification of the onset-of-acceleration.

Fig. 11 Area surrounding Vertical Array DT0014, as observed during the on-site inspection following the recorded critical event

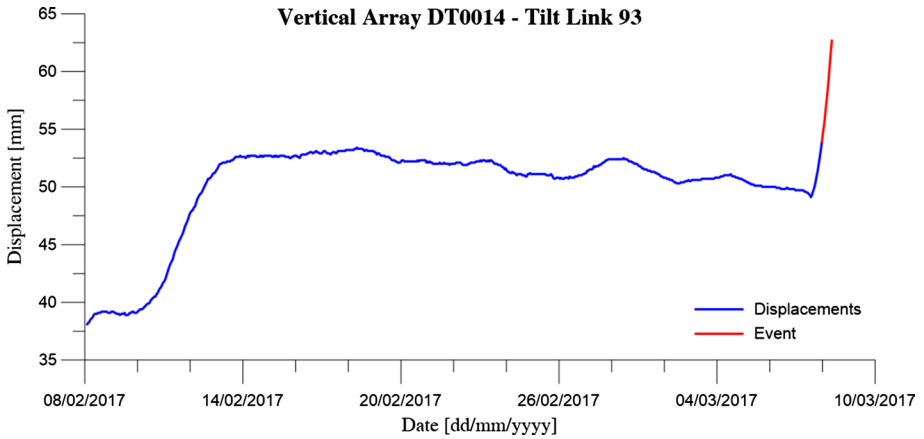

Fig. 12 Displacement values measured by Vertical Array DT0014—Tilt Link 93, referred to the event with OOA on 08/03/2017 02:28 AM, and to the 30 days preceding the event itself

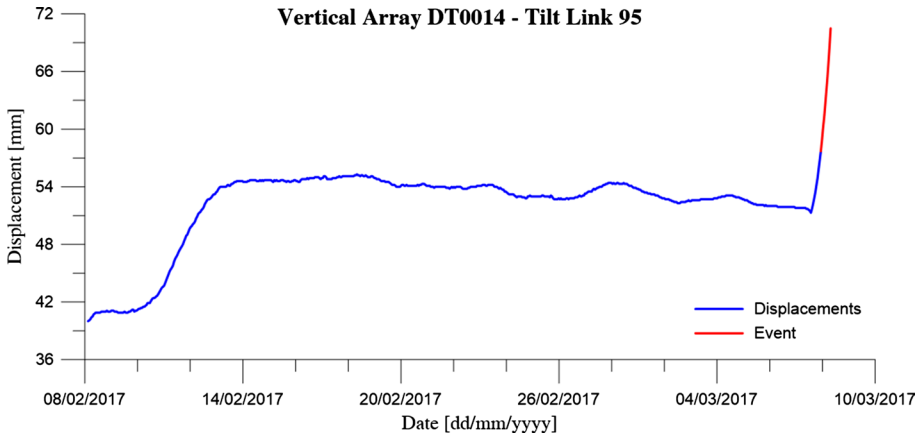

Fig. 13 Displacement values measured by Vertical Array DT0014—Tilt Link 95, referred to the event with OOA on 08/03/2017 02:28 AM, and to the 30 days preceding the event itself

Nonetheless, both datasets still showed a significant slope movement, with Tilt Link 93 recording 7.3 mm of displacement over a time period of 7 h, while displacements measured by Tilt Link 95 reached a value of 11.2 mm over the same time window.

As in previous cases, the available monitoring data were processed in order to evaluate the displacement measured by each Link during the event, and to assess the corresponding alert threshold. Given the one-hour sampling frequency of the Vertical Array, and since the detected event involved seven monitoring values, the 30-day time window provided 661 displacement values for each Tilt Link. The outcomes of this procedure are summarized in Table 8, and the graphical representation of the obtained value is displayed in Figs. 14 and 15. It is possible to notice how the event caused a displacement that clearly overcomes the threshold value for both datasets, thus confirming that the monitored phenomenon is showing a critical behavior. It is worth noting that this is the only confirmed slope collapse

Table 8 Features of the DT0014 Tilt Links and the datasets involved in the analysis, together with the displacement generated by the event and the equivalent displacement threshold

Tilt Link ID	Depth (m)	Dataset dimension k	Displacement generated d_0^* (mm)	Mean μ_s (mm)	Standard deviation σ_s (mm)	Equivalent displacement threshold d_{th}^* (mm)
93	2.50	7	7.3	0.31	0.51	1.9
95	1.80	7	11.2	0.34	0.67	2.4

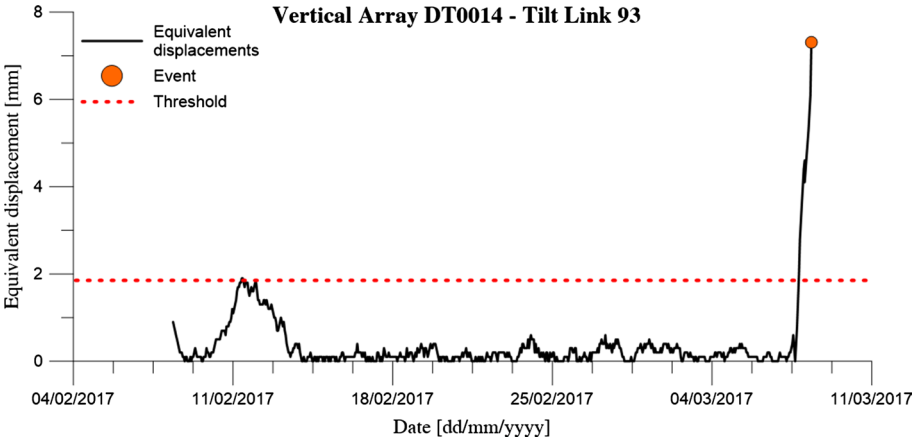

Fig. 14 Graphical representation of equivalent displacements referred to the event of interest, the time period of 30 days preceding the event itself, and the threshold evaluated from these values for DT0014—Tilt Link 93

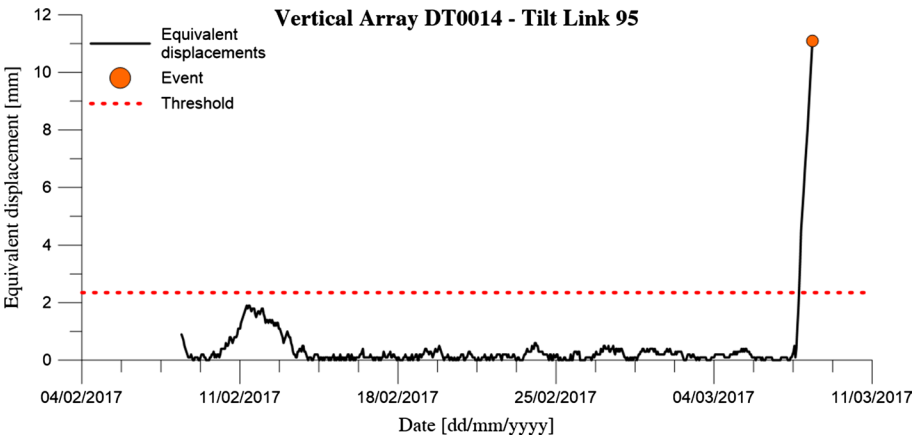

Fig. 15 Graphical representation of equivalent displacements referred to the event of interest, the time period of 30 days preceding the event itself, and the threshold evaluated from these values for DT0014—Tilt Link 95

recorded by MUMS inclinometers to date. An additional observation concerning this case study involves the results deriving from the application of a failure forecasting model, specifically the linear Inverse Velocity Method (Fukuzono 1985). The time of failure evaluated with this methodology was compared to the date of collapse observed from monitoring data (i.e., the date and time where instrumental data evidenced the damage caused to the Array by soil deformations). As reported by Segalini et al. (2019), both datasets provided a positive prediction of the slope collapse, with a time difference of 3 h for Tilt Link 93, and 1 h for Tilt Link 95.

4 Conclusions

The importance and effectiveness of Landslide Early Warning Systems has increased considerably over the years, thanks to the introduction of technological developments that allowed to improve their functionality and efficiency. One of the most important elements in a LEWS is represented by failure forecasting and alert thresholds assessment procedures, which represents an essential reference to identify slope instabilities and behaviors potentially leading to collapses and failures. In particular, the correct definition of alert levels should aim to minimize the occurrence of both false positive and missed alerts.

This paper deals with this issue by proposing a procedure to assess alert thresholds based on the concept of equivalent displacements, defined as the displacements generated in a time interval equal to the one showed by a specific event identified by the elaboration software. When referred to data sampled prior to the event of interest, they can give an indication of the past behavior of the monitored element. Therefore, they are able to establish a term of comparison in order to understand if the recorded event generated a displacement which does not correspond to a critical occurrence if compared to the entity of previously observed events, despite being geometrically compatible with an accelerating pattern. In order to achieve this objective, the approach here described involves the retrieval of monitoring values sampled in a time window of 30 days preceding the event of interest. These data are exploited to evaluate the equivalent displacements values, taking as a reference the duration of the detected event. Finally, the software is able to assess a threshold value on the basis of the mean and standard deviation values of the reference dataset.

Several examples are included in this paper, underlining the ability of the proposed model to define an effective threshold value to compare the potentially critical event with previously observed trends. In particular, the case studies here presented featured the on-site implementation of automatic monitoring instrumentation that provided an adequate amount of data to apply the methodology. The events here analyzed involve three events that did not lead to any significant effect on the stability conditions, and an occurrence where a collapse was observed following the development of significant slope deformations.

The results obtained can be summarized as follows:

– The exploitation of automatic instrumentation played an essential role in providing an appropriate amount of monitoring data for the application of the proposed methodology, giving also the possibility to implement the algorithm in the elaboration process with a near-real-time approach

- The model parameters selected during the model calibration process (i.e., dataset dimension, number of standard deviations) proved to be effective for the methodology implementation in a real case application
- The outcome of the threshold definition process applied to potentially critical events allowed to assess if the detected occurrence displayed a significant deviation from the standard behavior of the monitored slope, identifying also any false alarm generated by displacement trends geometrically compatible with an accelerating pattern

The methodology here presented successfully achieved the purpose of this paper, providing an effective and easily applicable procedure for the analysis of potentially critical events and the identification of false alarms. Nonetheless, since the monitoring of slope displacements is only one aspect of a very complex phenomenon, this model should not be applied in isolation. In fact, the most reliable approach should involve the integration of multiple methodologies in order to have a more complete description of the slope evolution over time.

Following the observations previously presented, it is worth mentioning some final considerations on the future developments involving the method here described. In particular, it would be interesting to apply the algorithm to other monitoring devices integrating automatic sampling operations in order to verify its adaptability to different landslide survey approaches. Moreover, another aspect that could be further investigated involves the possibility to exploit the proposed procedure to assess more than a single threshold. This could be achieved by varying the number of standard deviations considered in the equation used to evaluate the d^*_{th} value, in order to obtain different alert levels based on the landslide behavior and integrate appropriate safety measures according to the level reached.

Funding Open access funding provided by Università degli Studi di Parma within the CRUI-CARE Agreement. The authors declare that no funds were received during the preparation of this manuscript.

Declarations

Conflict of interest The authors have no conflicts of interest to declare that are relevant to the content of this paper.

References

Barla M, Antolini F (2016) An integrated methodology for landslides' early warning systems. Landslides 13:215–228. https://doi.org/10.1007/s10346-015-0563-8

Brox D, Newcomen W (2003) Utilizing strain criteria to predict highwall stability performance. In: Proceedings of the 10th ISRM Congress. OnePetro, Sandton, South Africa

Calvello M, d'Orsi RN, Piciullo L et al (2015) The Rio de Janeiro early warning system for rainfall-induced landslides: analysis of performance for the years 2010–2013. Int J Disaster Risk Reduct 12:3–15. https://doi.org/10.1016/j.ijdrr.2014.10.005

Carlà T, Macciotta R, Hendry M et al (2018) Displacement of a landslide retaining wall and application of an enhanced failure forecasting approach. Landslides 15:489–505. https://doi.org/10.1007/s10346-017-0887-7

Carri A, Chiapponi L, Giovanelli R et al (2015) Improving landslide displacement measurement through automatic recording and statistical analysis. Procedia Earth Planet Sci 15:536–541. https://doi.org/10.1016/j.proeps.2015.08.091

Chen H, Zeng Z, Tang H (2015) Landslide deformation prediction based on recurrent neural network. Neural Process Lett 41:169–178. https://doi.org/10.1007/s11063-013-9318-5

Crosta GB, Agliardi F (2002) How to obtain alert velocity thresholds for large rockslides. Phys Chem Earth Parts ABC 27:1557–1565. https://doi.org/10.1016/S1474-7065(02)00177-8

Di Biagio E, Kjekstad O (2007) Early warning, instrumentation and monitoring landslides. In: Proceedings of the 2nd regional training course, RECLAIM II. Phuket, Thailand

Di Napoli M, Carotenuto F, Cevasco A et al (2020) Machine learning ensemble modelling as a tool to improve landslide susceptibility mapping reliability. Landslides 17:1897–1914. https://doi.org/10.1007/s10346-020-01392-9

Du W, Wang G (2016) A one-step Newmark displacement model for probabilistic seismic slope displacement hazard analysis. Eng Geol 205:12–23. https://doi.org/10.1016/j.enggeo.2016.02.011

Fathani TF, Karnawati D, Wilopo W (2016) An integrated methodology to develop a standard for landslide early warning systems. Nat Hazards Earth Syst Sci 16:2123–2135. https://doi.org/10.5194/nhess-16-2123-2016

Festl J, Thuro K (2016) Determination of thresholds at the Aggenalm landslide (Bayrischzell, Germany) by time series analysis and numerical modeling. In: Aversa S, Cascini L, Picarelli L, Scavia C (eds) Landslides and engineered slopes. Experience, theory and practice. CRC Press, Boca Raton, pp 909–916

Fukuzono T (1985) A new method for predicting the failure time of a slope. In: Proceedings of the fourth international conference and field workshop on landslides. Tokyo University Press, Tokio, pp 145–150

Guardiani C, Soranzo E, Wu W (2021) Time-dependent reliability analysis of unsaturated slopes under rapid drawdown with intelligent surrogate models. Acta Geotech. https://doi.org/10.1007/s11440-021-01364-w

Guzzetti F, Peruccacci S, Rossi M, Stark CP (2007) Rainfall thresholds for the initiation of landslides in central and southern Europe. Meteorol Atmospheric Phys 98:239–267. https://doi.org/10.1007/s00703-007-0262-7

Huggel C, Khabarov N, Obersteiner M, Ramírez JM (2010) Implementation and integrated numerical modeling of a landslide early warning system: a pilot study in Colombia. Nat Hazards 52:501–518. https://doi.org/10.1007/s11069-009-9393-0

Intrieri E, Gigli G (2016) Landslide forecasting and factors influencing predictability. Nat Hazards Earth Syst Sci 16:2501–2510. https://doi.org/10.5194/nhess-16-2501-2016

Intrieri E, Gigli G, Casagli N, Nadim F (2013) Brief communication "landslide early warning system: toolbox and general concepts." Nat Hazards Earth Syst Sci 13:85–90. https://doi.org/10.5194/nhess-13-85-2013

Intrieri E, Carlà T, Gigli G (2019) Forecasting the time of failure of landslides at slope-scale: a literature review. Earth-Sci Rev 193:333–349. https://doi.org/10.1016/j.earscirev.2019.03.019

Liu Z, Gilbert G, Cepeda JM et al (2021) Modelling of shallow landslides with machine learning algorithms. Geosci Front 12:385–393. https://doi.org/10.1016/j.gsf.2020.04.014

Londoño CG (2011) Mountain risk management: integrated people centred early warning system as a risk reduction strategy, Northern Italy. Doctoral thesis, Università degli Studi di Milano-Bicocca, Department of Environmental and Territorial Sciences, Faculty of Mathematical, Physical and Natural Sciences

López-Vinielles J, Fernández-Merodo JA, Ezquerro P et al (2021) Combining satellite insar, slope units and finite element modeling for stability analysis in mining waste disposal areas. Remote Sens 13:2008. https://doi.org/10.3390/rs13102008

Ma Z, Mei G, Prezioso E et al (2021) A deep learning approach using graph convolutional networks for slope deformation prediction based on time-series displacement data. Neural Comput Appl. https://doi.org/10.1007/s00521-021-06084-6

Manconi A, Giordan D (2016) Landslide failure forecast in near-real-time. Geomat Nat Hazards Risk 7:639–648. https://doi.org/10.1080/19475705.2014.942388

Newcomen W, Dick G (2016) An update to the strain-based approach to pit wall failure prediction and a justification for slope monitoring. J South Afr Inst Min Metall 116:379–385. https://doi.org/10.17159/2411-9717/2016/v116n5a3

Pecoraro G, Calvello M, Piciullo L (2019) Monitoring strategies for local landslide early warning systems. Landslides 16:213–231. https://doi.org/10.1007/s10346-018-1068-z

Prakash N, Manconi A, Loew S (2021) A new strategy to map landslides with a generalized convolutional neural network. Sci Rep 11:9722. https://doi.org/10.1038/s41598-021-89015-8

Segalini A, Chiapponi L, Pastarini B, Carini C (2014) Automated inclinometer monitoring based on micro electro-mechanical system technology: applications and verification. In: Sassa K, Canuti P, Yin Y (eds) Landslide science for a safer geoenvironment. Springer, Cham, pp 595–600

Segalini A, Carri A, Valletta A, Martino M (2019) Innovative monitoring tools and early warning systems for risk management: a case study. Geosci 9:62. https://doi.org/10.3390/geosciences9020062

Thiebes B, Bell R, Glade T et al (2014) Integration of a limit-equilibrium model into a landslide early warning system. Landslides 11:859–875. https://doi.org/10.1007/s10346-013-0416-2

UNISDR (2006) Developing early warning systems, a checklist. In: third international conference on early warning (EWC III). Bonn, Germany

UNISDR (2009) UNISDR terminology on disaster risk reduction Switzerland Geneva

United Nations (2016) Report of the open-ended intergovernmental expert working group on indicators and terminology relating to disaster risk reduction

Valletta A, Segalini A, Carri A (2020) Application of a generalized criterion: time-of-failure forecast and alert thresholds assessment for landslides. In: De Maio M, Tiwari AK (eds) Applied geology: approaches to future resource management. Springer, Cham, pp 283–298

Valletta A, Carri A, Segalini A (2021) Definition and application of a multi-criteria algorithm to identify landslide acceleration phases. Georisk Assess Manag Risk Eng Syst Geohazards 16:1–15. https://doi.org/10.1080/17499518.2021.1952610

Xu Q, Yuan Y, Zeng Y, Hack R (2011) Some new pre-warning criteria for creep slope failure. Sci China Technol Sci 54:210–220. https://doi.org/10.1007/s11431-011-4640-5

Zhang X, Zhu C, He M et al (2022) Failure mechanism and long short-term memory neural network model for landslide risk prediction. Remote Sens 14:166. https://doi.org/10.3390/rs14010166

Zhao B, Dai Q, Han D et al (2020) Application of hydrological model simulations in landslide predictions. Landslides 17:877–891. https://doi.org/10.1007/s10346-019-01296-3